Silvo ROPOŠA[1], Gorazd ŠTUMBERGER[2], Darko LESTAN[3], Miran ROŠER[4]

Elektro Maribor d.d. (1), University of Maribor (2), Altens d.o.o. (4), Elektro Celje d.d. (4)

Application of voltage stabilizer in Slovenian low voltage grid

Abstract. In a competitive market power utilities are putting a lot of efforts in meeting vast range of customers' expectations in order to secure their market share. Their responsibility to provide adequate voltage quality throughout their grid is most important. A new type of voltage booster (MVB) is available on the Slovenian market since 2008. It is installed in the low voltage distribution line before consumers with poor voltage level. It raises the voltage at the output to a pre-set level of 235V and keeps it stable in spite of vast variations of power consumption. In this paper electrical characteristics of the MVB are analysed through the orthogonal decomposition of currents and also through power quality measurements analysis, taking into consideration SIST EN 50160 standard.

Streszczenie. Na konkurencyjnym rynku instytucji energetycznych duży nacisk jest położony na realizacje wysokich wymagań klientów, aby zapewnić ich udział w udziałach rynkowych. Odpowiedzialność w dostarczaniu odpowiedniej jakości napięcia przez własną sieć jest dla każdego operatora bardzo ważna. Nowy tym napięciowego wzmacniacza jest dostępny na rynku słoweńskim od 2008 roku. Jest on instalowany w liniach rozdzielczych niskiego napięcia o słabym poziomie napięcia. Podnosi napięcie na wyjściu do 235V i utrzymuje je stabilne pomimo bogatej zmienności w konsumowaniu energii. W artykule przeanalizowano charakterystykę tego wzmacniacza przez dokonanie ortogonalnej dekompozycji prądów, jak również przez analizę pomiarową jakości mocy. (Zastosowanie stabilizatora napięcia w słoweńskiej sieci elektroenergetycznej)

Keywords: voltage stabilizer, magnetically controllable inductance, low voltage distribution network.
Słowa kluczowe: stabilizator napięcia, sterowana magnetycznie indukcyjnośc, sieć rozdzielcza niskonapięciowa

Introduction

The voltage boosters like discussed Magtech device, represent a fast and economically acceptable solution for improving voltage conditions in the low voltage distribution networks where voltage level is insufficient. After installing the voltage booster in the network, the voltage and current levels on the primary and as well as on the secondary - consumer side of the installed booster change. Magtech voltage boosters are capable to eliminate most problems related with the amplitudes of supply voltages at the costumers' side. However, they behave as nonlinear loads deteriorating waveforms of the output voltages and currents.

All nonlinear loads increase total harmonic distortion of currents and voltages and increase losses related with the energy transmission [1]–[4]. In this paper electrical characteristics of the MVB are analyzed [5]. Due to the presence of higher order harmonic components in measured signals, an analysis based on the orthogonal decomposition of currents in time domain has been performed. In order to perform harmonic analysis the Fourier analysis has been applied.

MCI – magnetically controllable inductance

Thanks to the application of a magnetically controllable inductance MCI, step-less voltage regulation within the MVB is made possible without any moving parts or any semiconductors in the power circuit. This technology makes MVB a fast responsive, robust and no-maintenance device with a long lifespan.

The MCI is produced with sole copper and iron. The main copper winding on the outside produces alternate magnetic flux within the core. A hidden DC control winding on the inside produces a steady magnetic flux, which is perpendicular to the main one. The amount of DC flux sets the inductance value in the main winding. MCI is a magnetically adjustable inductor with an exceptional efficiency and large control range.

MVB design layouts and basic operation principle

Basic circuit diagram of a single phase voltage booster is shown in Fig. 1. The circuit consists out of the autotransformer '*A*' with a serial winding '*S*' connected between input point L_i and output point L_o of the voltage boosting circuit and parallel winding '*P*', which is parallel to the input. There is also a variable inductance 'L_{MCI}' in parallel to the input. For the reasons of clarity, all control circuits are omitted in Fig. 1.

In the single-phase electric system shown in Fig. 1, where current and voltage contain only fundamental order harmonic components, boosting can be explained through two simple circuit equations using phasors:

(1) $$\underline{U}_i = \underline{U}_{MCI} + \underline{U}_P$$

(2) $$\underline{U}_o = \underline{U}_{MCI} + \underline{U}_P + \underline{U}_S = \underline{U}_i + \underline{U}_S$$

where $\underline{U}_i$ and $\underline{U}_o$ are the phasors of input and output voltages, $\underline{U}_P$ and $\underline{U}_S$ are the phasors of voltages on the parallel and on the serial windings, wile $\underline{U}_{MCI}$ is the phasor of voltage on the variable inductance L_{MCI}.

The pre-set output value $\underline{U}_o$ is fixed to 235V. All the variations of the input voltage $\underline{U}_i$ must be, therefore, compensated by dynamically adjusting the circuit characteristics. Since the autotransformer ratio is not variable but fixed, the voltage adjustment could only be performed by changing the inductivity of the L_{MCI} ('*B*').
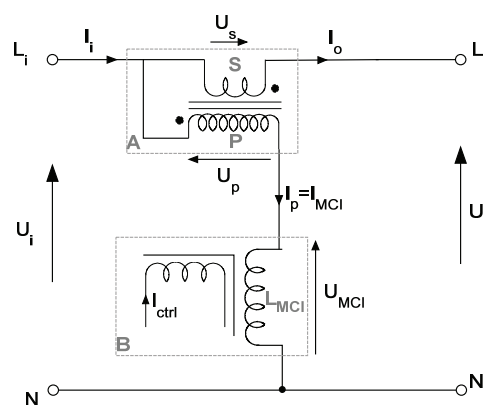

Fig.1. Basic circuit representation of a single-phase voltage booster

In Fig. 1 $\underline{I}_i$ and $\underline{I}_o$ are the phasors of input and output currents, while $\underline{I}_p$ (=$\underline{I}_{MCI}$) is the phasor of current in parallel winding. I_{ctrl} is DC current for induction of a perpendicular magnetic flux. With the "*N*" the neutral point of MVB is denoted.

There are many known types of variable inductances. The specifics of the MCI are shown in Fig. 2. There is no mechanical movement or geometry change involved in inductivity variation. MCI exploits the so called "Virtual Air Gap Effect".

Alternate electric current I_p in main inductance winding induces the magnetic flux B_f. The inductivity of such an inductance is determined, among other factors, by the core permeability. Through the induction of a perpendicular magnetic flux $B_s = f(I_{ctrl})$ within the same magnetic core, permeability in the direction of B_f can be altered and thus inductivity changed.
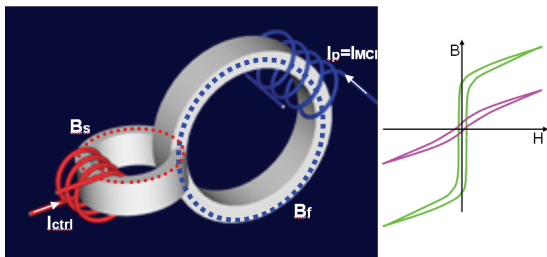

Fig.2. MCI and variable hysteresis

Orthogonal decomposition of currents in time domain
Let $u_1(t)$, $u_2(t)$ and $u_3(t)$ be the voltages and $i_1(t)$, $i_2(t)$ and $i_3(t)$ be the currents of the three-phase system observed over a selected time interval $t \in [0,T]$, where they can be treated as continious functions. In order to determine current necessary for energy transmission from the source to the load, presented in the form of active power P, current vector $\mathbf{i}$ and voltage vector $\mathbf{u}$ are introduced by (3).

$$(3) \qquad \mathbf{u} = \begin{bmatrix} u_1(t) \\ u_2(t) \\ u_3(t) \end{bmatrix}, \qquad \mathbf{i} = \begin{bmatrix} i_1(t) \\ i_2(t) \\ i_3(t) \end{bmatrix}$$

The inner product of both vectors is introduced by (4).

$$(4) \qquad \begin{aligned} (\mathbf{u},\mathbf{i}) &= \frac{1}{T}\int_0^T \mathbf{u}^T \mathbf{i}\, \mathrm{d}t = \\ &= \frac{1}{T}\int_0^T (u_1(t)i_1(t) + u_2(t)i_2(t) + u_3(t)i_3(t))\mathrm{d}t = \\ &= P_1 + P_2 + P_3 = P \end{aligned}$$

where P_1, P_2 and P_3 are active powers of individual phases, wile P is the active power for the entire three-phase system. In the similar way squares of the current vector norm $\|\mathbf{i}\|^2$ and voltage vector norm $\|\mathbf{u}\|^2$ are introduced by (5) and (6), respectively:

$$(5) \qquad \begin{aligned} \|\mathbf{i}\|^2 &= (\mathbf{i},\mathbf{i}) = \frac{1}{T}\int_0^T \mathbf{i}^T \mathbf{i}\, \mathrm{d}t = \\ &= \frac{1}{T}\int_0^T (i_1^2(t) + i_2^2(t) + i_3^2(t))\mathrm{d}t = I_1^2 + I_2^2 + I_3^2 \end{aligned}$$

$$(6) \qquad \begin{aligned} \|\mathbf{u}\|^2 &= (\mathbf{u},\mathbf{u}) = \frac{1}{T}\int_0^T \mathbf{u}^T \mathbf{u}\, \mathrm{d}t = \\ &= \frac{1}{T}\int_0^T (u_1^2(t) + u_2^2(t) + u_3^2(t))\mathrm{d}t = U_1^2 + U_2^2 + U_3^2 \end{aligned}$$

where the squares of RMS values of currents and voltages in individual phases are denoted by I_1^2, I_2^2, I_3^2 and U_1^2, U_2^2, U_3^2.

The current vector $\mathbf{i}$ (3) can be decomposed into two orthogonal components. The first one, denoted with $\mathbf{i}_u$ (7),

represents the current vector component aligned with the voltage vector $\mathbf{u}$ (3). The current vector $\mathbf{i}_u$ is indispensable for energy transmission from the source to the load, represented in the form of active power P.

The second vector component, denoted with $\mathbf{i}_{uo}$ (8), is orthogonal to the voltage vector $\mathbf{u}$ (3) and does not contribute to the active power P.

$$(7) \qquad \mathbf{i}_u = \begin{bmatrix} i_{1u} \\ i_{2u} \\ i_{3u} \end{bmatrix} = \frac{P}{\|\mathbf{u}\|^2}\mathbf{u}$$

$$(8) \qquad \mathbf{i}_{uo} = \begin{bmatrix} i_{1uo} \\ i_{2uo} \\ i_{3uo} \end{bmatrix} = \mathbf{i} - \mathbf{i}_u$$

The current vector components $\mathbf{i}_u$ and $\mathbf{i}_{uo}$ are orthogonal, which means, that their inner product equals zero (9).

$$(9) \qquad (\mathbf{i}_u, \mathbf{i}_{uo}) = 0$$

The norms of vector $\mathbf{i}$ and its orthogonal components $\mathbf{i}_u$ and $\mathbf{i}_{uo}$ are related by (10). The square of current vector norm is defined in (5). In the similar way squares of the current vector norms $\|\mathbf{i}_u\|^2$ and $\|\mathbf{i}_{uo}\|^2$ are introduced by (11) and (12), respectively:

$$(10) \qquad \|\mathbf{i}\|^2 = \|\mathbf{i}_u\|^2 + \|\mathbf{i}_{uo}\|^2$$

$$(11) \qquad \begin{aligned} \|\mathbf{i}_u\|^2 &= (\mathbf{i}_u, \mathbf{i}_u) = \frac{1}{T}\int_0^T \mathbf{i}_u^T \mathbf{i}_u\, \mathrm{d}t = \\ &= \frac{1}{T}\int_0^T (i_{u1}^2(t) + i_{u2}^2(t) + i_{u3}^2(t))\mathrm{d}t \end{aligned}$$

$$(12) \qquad \begin{aligned} \|\mathbf{i}_{uo}\|^2 &= (\mathbf{i}_{uo}, \mathbf{i}_{uo}) = \frac{1}{T}\int_0^T \mathbf{i}_{uo}^T \mathbf{i}_{uo}\, \mathrm{d}t = \\ &= \frac{1}{T}\int_0^T (i_{uo1}^2(t) + i_{uo2}^2(t) + i_{uo3}^2(t))\mathrm{d}t \end{aligned}$$

The instantaneous powers are defined by (13), where $s(t)$, $p(t)$ and $q(t)$ are the apparent, active and reactive instantaneous powers of the three-phase system, respectively.

$$(13) \qquad \begin{aligned} s(t) &= \mathbf{u}^T(t)\mathbf{i}(t) \\ p(t) &= \mathbf{u}^T(t)\mathbf{i}_u(t) \\ q(t) &= \mathbf{u}^T(t)\mathbf{i}_{uo}(t) \end{aligned}$$

The squares of three-phase input and output apparent, active and reactive average powers are defined by (14).

$$(14) \qquad \begin{aligned} S^2(t) &= \|\mathbf{i}(t)\|_2^2 \|\mathbf{u}(t)\|_2^2 \\ P^2(t) &= \|\mathbf{i}_u(t)\|_2^2 \|\mathbf{u}(t)\|_2^2 \\ Q^2(t) &= \|\mathbf{i}_{uo}(t)\|_2^2 \|\mathbf{u}(t)\|_2^2 \end{aligned}$$

The generalized power factor PF' is defined by (15).

$$(15) \qquad PF' = \frac{\|\mathbf{i}_u\|}{\|\mathbf{i}\|} = \frac{\|\mathbf{i}_u\|\|\mathbf{u}\|}{\|\mathbf{i}\|\|\mathbf{u}\|} = \frac{|P|}{\|\mathbf{i}\|\|\mathbf{u}\|}$$

The total harmonic distortions of individual line voltages THD_U are defined by (16).

$$(16) \qquad THD_U = \frac{\sum_{h=2}^{40} U_h^2}{U_1^2}$$

where U_h denotes the RMS values of voltage harmonic components of order h, while U_1 denote the RMS value of fundamental harmonic voltage.

Results

In this chapter, the results of measurements and analysis are presented. All results presented are given for MVB with rated power 55kVA. Fig. 3 shows voltage level U_{mean} in the form of root mean square value of the line voltage and voltage total harmonic distortion THD_U over the first week of MVB operation.
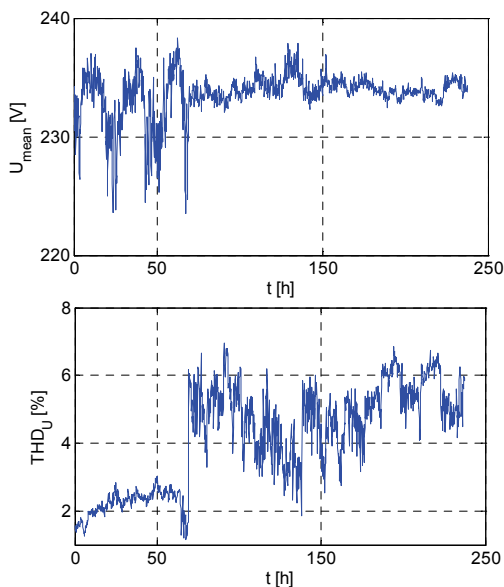
Fig.3. Voltage and **THD**$_U$ of the phase L$_2$ at the MVB output

There is a visible change in values at the exact moment when MVB was first activated. Voltages on the MVB output were stabilized but on the other hand, a noticeable increase of *THD* appeared as well, although the SIST EN50160 allowed limits (8 %) were not exceeded.

Fig. 4 and 5 shows phase L_2 input and output voltages (u_i, u_o) and currents (i_i, i_o).
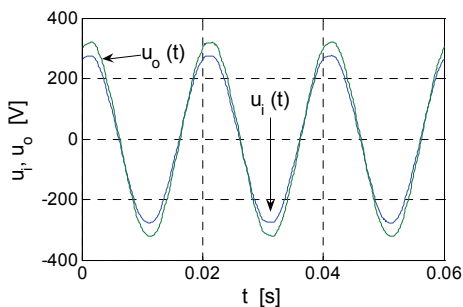

Fig.4. L$_2$ voltage at the MVB input (i) and output (o)
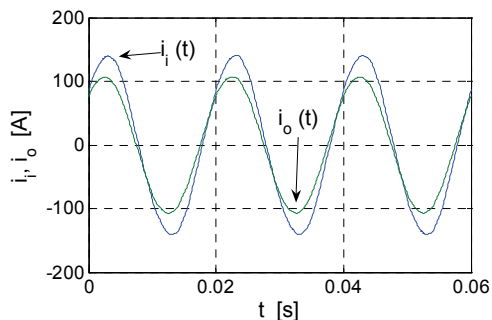

Fig.5. L$_2$ current at the MVB input (i) and output (o)

As declared through the basic MVB functionality, output voltage is higher when comparing to the input. Also as expected, the input current is increased since input power balances with the output.

Figs. 6 and 7 shows input and output currents of the MVB together with their orthogonal components. Comparison of orthogonal components exposes the main difference between input and output, which lies in the current vector $\mathbf{i}_{uo}$ (8). On the other hand, current vector $\mathbf{i}_u$ (7) shows very little or no difference between input and output. This situation indicates low active power loss and higher reactive power losses through the MVB as a consequence of MVB being an inductive load to a generator (i.e. upstream network). Apparent, active and reactive power can be calculated by equation (13).
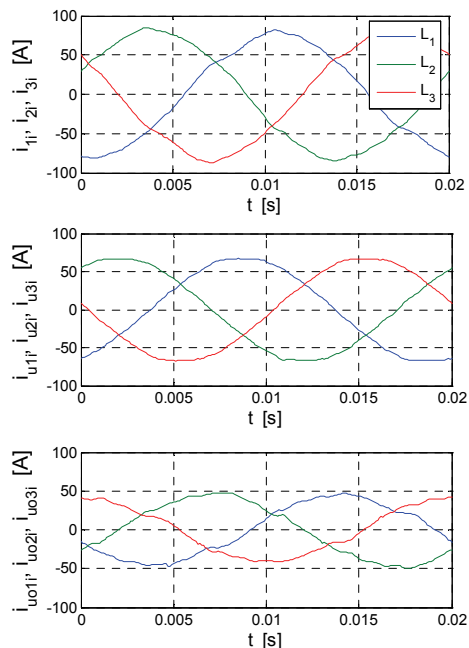

Fig.6. Orthogonal decomposition of MVB input currents

In Figs. 6 and 7 i_{1i}, i_{2i}, i_{3i} and i_{1o}, i_{2o}, i_{3o} are the measured input (i) and output (o) currents of MVB. Similarly, i_{u1i}, i_{u2i}, i_{u3i} and i_{u1o}, i_{u2o}, i_{u3o} are the input and output currents aligned with the voltages, calculated by (7), while i_{uo1i}, i_{uo2i}, i_{uo3i} and i_{uo1o}, i_{uo2o}, i_{uo3o} are the input and output currents orthogonal to the voltages, calculated by (8).
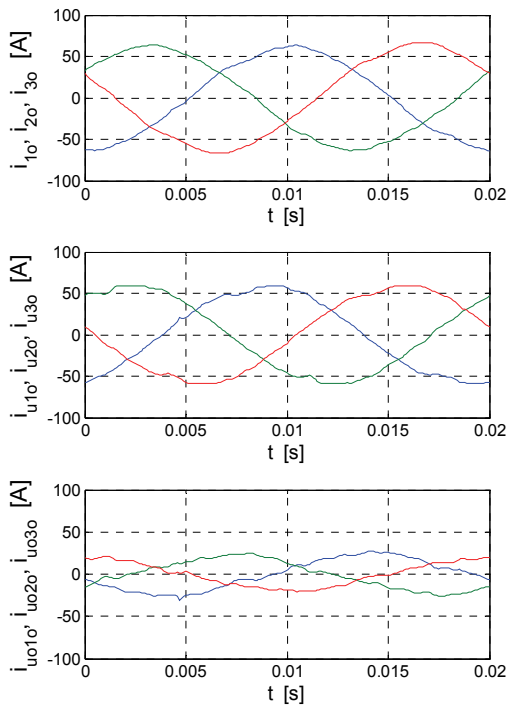
Fig.7. Orthogonal decomposition of MVB output currents

Fig. 8 show three-phase input and output apparent power, reactive power, all as functions of active input power of the voltage booster.
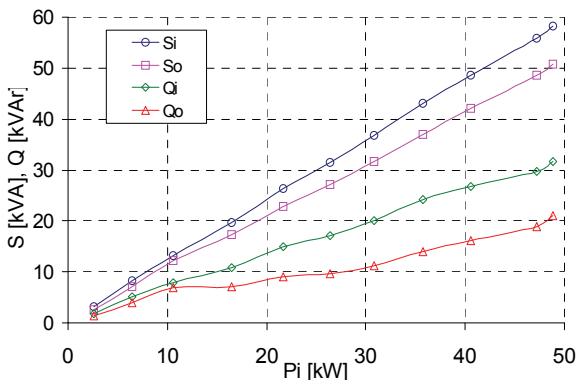

Fig.8. Input and output powers of the MVB under different loads

Tree-phase apparent, active and reactive powers shown in Fig. 8 by (13) are determined. S_i and Q_i represent input apparent and reactive power of the MVB, while S_o and Q_o represent output apparent and reactive power of the MVB. P_i is active power at the MVB input.

Fig. 9 show total harmonic distortion THD_U as function of active input power of the voltage booster. For the THD characteristic the Fourier analysis has been applied. Total harmonic distortion THD_U shown in Fig. 9 by (16) is determined.
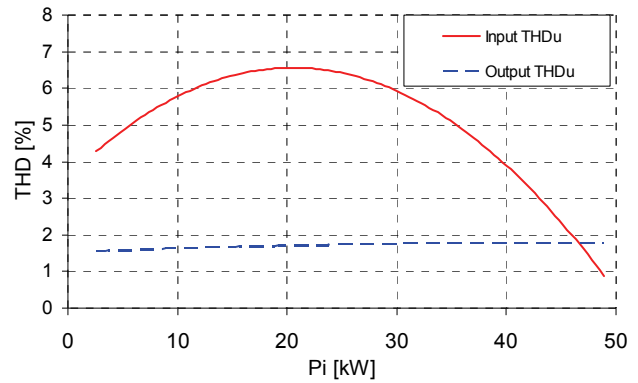

Fig.9. THD_U of the MVB under different loads

Conclusion

Field measurement clearly shows that the voltage booster is perfectly capable of maintaining constant output voltage disregarding the load variations with app. 200ms response time. Due to the circuit configuration (Fig. 1), the input power factor is decreased which slightly increases system power losses (Fig. 8). Fig. 9 clearly shows that the harmonic content significantly changes with the MVB boosting factor. Due to unbalanced three-phase system and presence of high order harmonics, orthogonal decomposition of currents in the time domain was used to evaluate the impact of the MVB on distribution network.

Following to the results, further knowledge and experience is gained on the applicability and fine tuning of future MVB installations.

REFERENCES
[1] S. Svensson, ''Power measurement uncertainties in a nonsinusoidal power system, International Symposium on Electric Power Engineering'', *Proceedings: Power systems, (Stockholm, Sweden), pp.617–622, IEEE, 1995*
[2] G. Štumberger, D. Dolinar, F. Gubina, B. Grčar, ''Orthogonal decomposition of currents and definition of power in three phase systems'', *Proceedings: Electrotechnical Review, volume 64, number 5, pp.288-295, 1997*
[3] J. L. Willems, "A new interpretation of the Akagi–Nabae power components for nonsinusoidal three–phase situations," IEEE Transactions on Instrumentation and Measurements, vol. 41, no. 4, pp. 523–527, 1992
[4] G. Štumberger, ''The treatment of three-phase systems using vector spaces'', Ph.D. Thesis, University of Maribor – Faculty of electrical engineering and computer science, Maribor, 1996
[5] Technical documentation of the producer Magtech AS, *Norway (www.Magtech.no)*

Authors: *Silvo Ropoša, Elektro Maribor d.d., Vetrinjska ul. 2, SI-2000 Maribor, Slovenia, E-mail: silvo.roposa@elektro-maribor.si; dr. Gorazd Štumberger, University of Maribor, Faculty of electrical engineering and computer science, Smetanova ul. 17, SI-2000 Maribor, Slovenia, E-mail: gorazd.stumberger@uni-mb.si; Darko Lestan, Altens d.o.o., Linhartova 13, SI-1000 Ljubljana, Slovenia, E-mail: info@altens.si; Miran Rošer, Elektro Celje d.d., Vrunčeva 2a, SI-3000 Celje, Slovenia, E-mail: miran.roser@elektro-celje.si.*